

Ultra-cold bosons in zig-zag optical lattices

S. Greschner,¹ L. Santos,¹ and T. Vekua¹

¹*Institut für Theoretische Physik, Leibniz Universität Hannover, 30167 Hannover, Germany*

Ultra-cold bosons in zig-zag optical lattices present a rich physics due to the interplay between frustration, induced by lattice geometry, two-body interaction and three-body constraint. Unconstrained bosons may develop chiral superfluidity and a Mott-insulator even at vanishingly small interactions. Bosons with a three-body constraint allow for a Haldane-insulator phase in non-polar gases, as well as pair-superfluidity and density wave phases for attractive interactions. These phases may be created and detected within the current state of the art techniques.

Introduction Atoms in optical lattices offer extraordinary possibilities for the controlled emulation and analysis of lattice models and quantum magnetism [1]. Various lattice geometries are attainable by means of proper laser arrangements, including triangular [2] and Kagome [3] lattices, opening fascinating possibilities for the study of geometric frustration, which may result in flat bands in which the constrained mobility may largely enhance the role of interactions [4]. Moreover, the value and sign of inter-site hopping may be modified by means of shaking techniques [5, 6], allowing for the study of frustrated antiferromagnets with bosonic lattice gases [7].

Interatomic interactions may be controlled basically at will by means of Feshbach resonances [8]. In particular, large on-site repulsion may allow for the suppression of double occupancy in bosonic gases at low fillings (hard-core regime). Interestingly, it has been recently suggested that, due to a Zeno-like effect, large three-body loss rates may result in an effective three-body constraint, in which no more than two bosons may occupy a given lattice site [9]. This constraint opens exciting novel scenarios, especially in what concerns stable Bose gases with attractive on-site interactions, including color superfluids in spinor Bose gases [10] and pair-superfluid phases [9, 11, 12]. The suppression of three-body occupation has been hinted in recent experiments [13].

Under proper conditions, lattice gases may resemble to a large extent effective spin models, e.g. hard-core bosons may be mapped into a spin-1/2 XY Heisenberg model [1]. Lattice bosons at unit filling resemble to a large extent spin-1 chains [14], and in the presence of inter-site interactions, as it is the case of polar gases [15], have been shown to present a gapped Haldane-like phase [16] (dubbed Haldane-insulator (HI) [14, 17]) characterized by a non-local string-order [18].

In this Letter we analyze the physics of ultra-cold bosons in zig-zag optical lattices. We show that the interplay of frustration and interactions lead to a different physics for unconstrained and constrained (with up to two particles per site) bosons. For unconstrained bosons, geometric frustration induces chiral superfluidity, and allows for a Mott-insulator phase even at vanishingly small interactions. For constrained bosons, we show

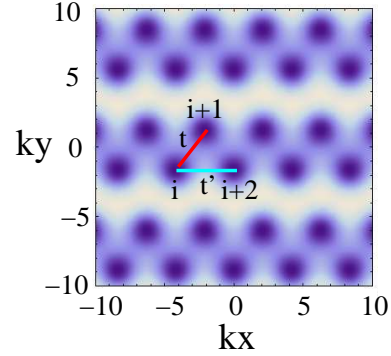


FIG. 1: Zig-zag chains formed by an incoherent superposition between a triangular lattice [2] $V_1(\vec{r} \equiv (x, y)) = V_{10} \left[\sin^2 \left(\vec{b}_1 \cdot \vec{r}/2 \right) + \sin^2 \left(\vec{b}_2 \cdot \vec{r}/2 \right) + \sin^2 \left((\vec{b}_1 - \vec{b}_2) \cdot \vec{r}/2 \right) \right]$, with k the laser wavenumber, $\vec{b}_1 = \sqrt{3}k\vec{e}_y$ and $\vec{b}_2 = \sqrt{3}k(\sqrt{3}\vec{e}_x/2 - \vec{e}_y/2)$, and an additional lattice $V_2(\vec{r}) = V_{20} \sin^2(\sqrt{3}ky/4 - \pi/4)$. In the figure, in which $V_{20}/V_{10} = 2$, darker regions mean lower potential. The hopping rate between nearest (next-nearest) neighbors is $t > (t')$.

that a Haldane-insulator phase becomes possible even for non-polar gases. Moreover, pair-superfluid [9, 11, 12] and density-wave phases may occur for attractive on-site interactions. A direct first-order phase transition from Haldane-insulator to pair-superfluid is observed and explained. These phases may be realized and detected with existing state of the art techniques.

Zig-zag lattices. In the following we consider bosons in zig-zag optical lattices. As shown in Fig. 1, this particular geometry may result from the incoherent superposition of a triangular lattice with elementary cell vectors $\vec{a}_1 = a\vec{e}_x$ and $\vec{a}_2 = a(\frac{1}{2}\vec{e}_x + \frac{\sqrt{3}}{2}\vec{e}_y)$ (formed by three laser beams of wavenumber $k = 4\pi/3a$ oriented at 120 degrees from each other, as discussed in Ref. [2]) and a superlattice with lattice spacing $\sqrt{3}a$ oriented along y . For a sufficiently strong superlattice, zig-zag ladders are formed, and the hopping between ladders may be neglected. We will hence concentrate in the following on the physics of bosons in a single zig-zag ladder, which is to a large extent given by the rates t and t' characterizing the hopping along the two directions $\vec{a}_{1,2}$ (Fig. 1). As shown in Ref. [7], a periodic lattice shaking may be employed to

control the value of t and t' independently. Interestingly, their sign may be controlled as well. In the following we consider an inverted sign for both hoppings, which result in an anti-ferromagnetic coupling between sites [7].

Model. Ordering the sites as indicated in Fig. 1, the physics of the system is given by a Bose-Hubbard Hamiltonian with on-site interactions characterized by the coupling constant U , nearest-neighbor hopping $t < 0$ and next-nearest-neighbor hopping $t' < 0$:

$$H = \sum_i \left[-\frac{t}{2} b_i^\dagger b_{i+1} - \frac{t'}{2} b_i^\dagger b_{i+2} + \text{H.c.} \right] + \frac{U}{2} \sum_i n_i(n_i - 1) + U_3 \sum_i n_i(n_i - 1)(n_i - 2), \quad (1)$$

where b_i^\dagger, b_i are the bosonic creation/annihilation operators of particles at site i , $n_i = b_i^\dagger b_i$, and we have added the possibility of three-body interactions, characterized by the coupling constant U_3 . We assume below an average unit filling $\bar{n} = 1$.

Unconstrained bosons. We discuss first the ground-state properties of unconstrained bosons ($U_3 = 0$). At $U = 0$, the Hamiltonian (1) is diagonalized in quasi-momentum space $H = \sum_k \epsilon(k) b_k^\dagger b_k$, with the dispersion $\epsilon(k) = |t|(\cos k + j \cos 2k)$, with $j \equiv t'/t$. Depending on the frustration j we may distinguish two regimes. If $j < 1/4$, the dispersion $\epsilon(k)$ presents a single minimum at $k = \pi$, and hence small U will introduce a superfluid (SF) phase, with quasi-condensate at $k = \pi$. If $j > 1/4$, $\epsilon(k)$ presents two non-equivalent minima at $k = k_0 \equiv \pm \arccos[-1/4j]$. As shown below, interactions favor the predominant population of one of these minima, and the system enters a chiral superfluid (CSF) phase with a non-zero local boson current characterized by a finite chirality $\langle \kappa_i \rangle$, with $\kappa_i = \frac{i}{2}(b_i^\dagger b_{i+1} - \text{H.c.})$. At $j = 1/4$, the Lifshitz point, the dispersion becomes quartic at the $k = \pi$ minimum, $\epsilon(k) \sim (k - \pi)^4$, the effective mass $m = (\partial^2 \epsilon(k) / \partial k^2)_{k=\pi}^{-1} = 1/t(1 - 4j)$ diverges, and even vanishingly small interactions become relevant.

To study the effect of interactions we combine numerical calculations based on the density matrix renormalization group (DMRG) method [25] (with up to $N = 300$ sites keeping per block on average 400 states for gapped phases and 600 states for gapless ones), and bosonization techniques to unveil the low-energy behavior of model (1). For $j < 1/4$, we employ standard bosonization transformations [19], with an additional oscillating factor $b_i \rightarrow (-1)^i e^{i\sqrt{\pi}\theta(x)}$, to obtain the low-energy effective theory, which is given by the sine-Gordon model

$$\mathcal{H} = \frac{v_s}{2} \left[\frac{(\partial_x \phi)^2}{K} + K(\partial_x \theta)^2 \right] - \mathcal{M} \cos[2\pi \bar{n}x - \sqrt{4\pi}\phi], \quad (2)$$

where θ and $\partial_x \phi$ describe phase and density fluctuations of bosons respectively, $[\theta(x), \partial_y \phi] = i\delta(x - y)$, v_s is the sound velocity and K the Luttinger parameter. In the

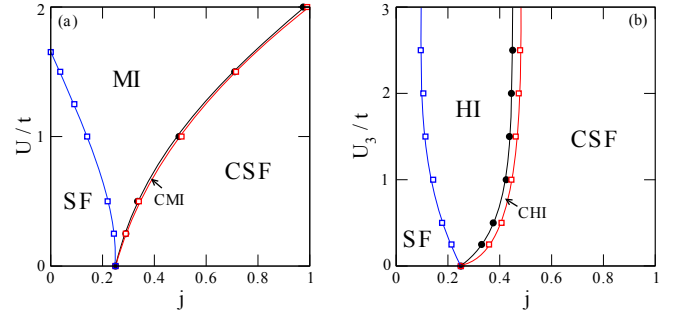


FIG. 2: Phase diagram for unconstrained bosons as a function of the frustration parameter j and (a) the on-site interaction U (with $U_3 = 0$) and (b) the three-body repulsion U_3 (and $U = 0$). In the figures, \bigcirc indicate the boundary of the chiral phases characterized by long-range ordered chirality-chirality correlations $\langle \kappa_i \kappa_j \rangle$; \square indicate the boundary of the SF-phases indicated by the critical Luttinger parameter $K = 2$. Note that narrow CMI and CHI phases may occur as well. For $U, U_3 \geq 0.5$ keeping $n_{max} = 4$ bosons per site in the DMRG-simulation can be shown to be sufficient.

weak-coupling, $Um \ll 1$, hydrodynamic relations are expected to hold: $v_s(j) \sim \sqrt{\bar{n}U/m\pi^2} = v_s(0)\sqrt{1-4j}$ and $K(j) \sim \sqrt{\bar{n}\pi^2/U m} = K(0)\sqrt{1-4j}$, clearly showing that j enhances correlations. At $j = 1/4$, m diverges and the system enters a Mott-insulator (MI) even for vanishingly small U (Fig. 2(a)). The SF-MI transition takes place however in the strong-coupling regime in which v_s and K must be determined numerically. We obtain K from the single-particle correlations $G_{ij} = \langle b_i b_j^\dagger \rangle$ which in the SF decay as $\sim (-1)^{i-j} |i-j|^{-1/2K}$. The value $K = 2$ marks the boundary between SF ($U < U_c$, $K > 2$) and MI ($U > U_c$, $K < 2$, and $\mathcal{M} > 0$). The MI phase is characterized by a hidden parity order [17], $\mathcal{O}_P^2 = \lim_{|i-j| \rightarrow \infty} \langle (-1)^{\sum_{i < l < j} \delta n_l} \rangle \sim \langle \cos \sqrt{\pi}\phi \rangle^2$, which has been recently measured in site-resolved experiments [20].

The $j > 1/4$ case is best understood from bosonization in the $j \gg 1$ regime. We may then introduce two pairs of bosonic fields (θ_1, ϕ_1) and (θ_2, ϕ_2) , describing, respectively, the subchains of even and odd sites. The effective model is governed by the Hamiltonian density

$$\mathcal{H} = \sum_{\alpha=\pm} \frac{v_\alpha}{2} \left[\frac{(\partial_x \phi_\alpha)^2}{K_\alpha} + K_\alpha (\partial_x \theta_\alpha)^2 \right] + \lambda \partial_x \theta_+ \sin \sqrt{2\pi} \theta_- - 2\mathcal{M} \cos \sqrt{2\pi} \phi_+ \cos \sqrt{2\pi} \phi_- \quad (3)$$

where $\theta_\pm = (\theta_1 \pm \theta_2)/\sqrt{2}$, $\phi_\pm = (\phi_1 \pm \phi_2)/\sqrt{2}$, v_\pm , K_\pm , and \mathcal{M} are phenomenological parameters (in the regimes displayed on Figure 2 (a)), $\lambda \sim j^{-1}$. Note that the chirality is given by $\kappa_i \rightarrow \sin \sqrt{2\pi} \theta_-(x)$. In weak-coupling, $Um' \ll 1$, with $m' = (\partial^2 \epsilon(k) / \partial k^2)_{k_0}^{-1} = 4j/t(16j^2 - 1)$, $v_\pm \sim \sqrt{\bar{n}U/m'\pi^2}$ and $K_\pm \sim \sqrt{\bar{n}\pi^2/U m'}$. In this case only the term $\partial_x \theta_+ \sin \sqrt{2\pi} \theta_-$ is relevant, resulting in $\langle \sin \sqrt{2\pi} \theta_- \rangle \neq 0$ [21]. Hence, a small U is expected to favor a CSF for $j > 1/4$, as our numerical results

confirm (Fig. 2(a)). The CSF phase is characterized by $G_{ij} \sim (-1)^{i-j} e^{-i\kappa(i-j)} |i-j|^{-1/4K_+}$, where $\kappa \sim \langle \kappa_i \rangle$.

Moreover, depending on the values of K_{\pm} bosonization opens the possibility of two consecutive phase transitions with increasing U starting from the CSF phase [22], which we have confirmed with our DMRG calculations (Fig. 2(a)). First a KT transition occurs from CSF to chiral-Mott (CMI), a narrow Mott phase with finite chirality. Then an Ising transition is produced from CMI to non-chiral MI. At both KT transition lines in Fig. 2(a) (SF-MI and CSF-CMI), up to a logarithmic prefactor, $G_{ij} \sim (-1)^{i-j} e^{-i\kappa(i-j)} |i-j|^{-1/4}$, where in CSF $\kappa \neq 0$.

Constrained bosons. As mentioned above, sufficiently large three-body losses may result in a three-body constraint $(b_i^\dagger)^3 = 0$ ($U_3 = \infty$) [9]. In that case, Model (1) may be mapped to a large extent onto a frustrated spin-1 chain model [23], which, presents the possibility of a gapped Haldane phase, characterized by a non-local string order. Hence, interestingly, constrained bosons in a zig-zag lattice may be expected to allow for the observation of the HI phase in the absence of polar interactions.

Indeed, a model with $U = 0$ and finite U_3 shows that at the Lifshitz point, $j = 1/4$, a HI phase is stabilized for arbitrarily weak U_3 (Fig. 2(b)). The effective theory describing the HI is again the sine-Gordon model (2) with $K < 2$. However, now $\mathcal{M} < 0$, which selects a hidden string order $\mathcal{O}_S^2 \equiv \lim_{|i-j| \rightarrow \infty} \langle \delta n_i \exp[i\pi \sum_{i < l < j} \delta n_l] \delta n_j \rangle \sim \langle \sin \sqrt{\pi} \theta \rangle^2$ [17]. Resembling the case of Fig. 2(a), SF, HI, chiral-HI (CHI) and CSF phases occur (Fig. 2(b)). These phases are expected for $U_3 = \infty$ from known results in frustrated spin-1 chains [27–29]. Our DMRG simulations suggest that all these phases meet at $j = 1/4$ for $U_3 \rightarrow 0$.

Figure 3 shows the phase diagram for constrained bosons ($U_3 = \infty$). Starting from the HI phase, increasing $U > 0$ can induce a Gaussian HI-MI phase transition, characterized by a vanishing $\mathcal{M} = 0$ in (2), resembling the phase transition between Haldane and large-D phases induced by single-ion anisotropy in spin-1 chains [30]. The SF phase is separated from the MI and HI by KT transitions, whereas at the CSF boundary with the MI (HI) a CMI (CHI) occurs as mentioned above (these very narrow regions are not resolved in Fig. 3).

Interestingly, constrained bosons allow as well for the exploration of attractive two-body interactions, $U < 0$, without collapse. The $U < 0$ phases are also depicted in Fig. 3. For sufficiently large $|U|$, bosons tend to cluster in pairs and, as already discussed in Ref. [9], for $j = 0$ an Ising transition between a SF and a pair superfluid (PSF) occurs [24], analogous to the XY1 to XY2 phase transition in spin-1 chains induced by single-ion anisotropy [30] (this transition has been recently studied for 2D lattices as well [11, 12]). The PSF phase is characterized by an exponentially decaying G_{ij} but algebraically decaying pair-correlation function $G_{ij}^{(2)} = \langle (b_i^\dagger)^2 (b_j)^2 \rangle$. Indeed

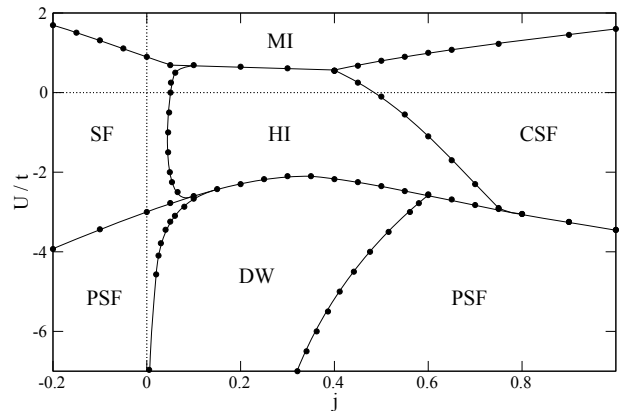


FIG. 3: Phase diagram for constrained bosons as a function of the on-site interaction U and the frustration parameter j . Narrow CMI and CHI phases may occur along the phase transition lines from CSF to MI and CSF to HI, respectively, but their extension would be negligible in the figure. For the precise location of the PSF-DW and HI-MI transition we have additionally analyzed the energy-level-crossings with, respectively, periodic and twisted-boundary conditions. The KT transitions from SF to MI and HI have been determined by the extraction of the Luttinger parameter K [26].

a PSF occurs for sufficiently large $|U|$, also for $j > 1/4$ which is characterized in bosonization in Eq. (3) by a gapped antisymmetric sector, with pinned ϕ_- , and a gapless symmetric sector [31]. Though one may anticipate an Ising phase transition between the CSF (with broken discrete parity symmetry) and the PSF (with restored symmetry), the behavior of \mathcal{O}_P^2 and κ (not shown) hints to a weakly first-order nature.

Small $U < 0$ disfavors singly-occupied sites and thus enhances \mathcal{O}_S^2 and the bulk excitation gap of the HI phase (see Figs. 4 and 5). However, since large $U < 0$ removes singly occupied sites completely, just like strong nearest neighbour repulsion, it is expected that the HI phase eventually will transform for growing $|U|$ into a gapped density-wave (DW) phase via Ising phase transition [14], and string order will evolve into DW order (Fig. 4 shows how \mathcal{O}_s merges with $\mathcal{O}_{DW} \equiv \lim_{j \rightarrow \infty} (-1)^j \langle n_i n_{i+j} \rangle$ for $U/t < -3$). The DW phase is characterized by an exponential decay of both G_{ij} and $G_{ij}^{(2)}$ though a finite \mathcal{O}_{DW} . Our DMRG results confirm this scenario (see Fig. 4), showing that a DW phase is located between the above mentioned PSF regions (Fig. 3).

Interestingly the DW phase remains in between both PSF regions all the way into $U \rightarrow -\infty$. In that regime, we may project out singly-occupied sites, and introduce a pseudo-spin-1/2, identifying $|0\rangle \rightarrow |\downarrow\rangle$, $|2\rangle \rightarrow |\uparrow\rangle$, and defining the spin operators $\tau_i^- \rightarrow (-1)^i b_i^2 / \sqrt{2}$, $2\tau_i^z \rightarrow b_i^\dagger b_i - 1$. The effective model to leading order in $1/|U|$ is a spin-1/2 chain:

$$H_{\frac{1}{2}} = J \sum_i [\tau_i \tau_{i+1} + j^2 (\tau_i^z \tau_{i+2}^z - \tau_i^x \tau_{i+2}^x - \tau_i^y \tau_{i+2}^y)], \quad (4)$$

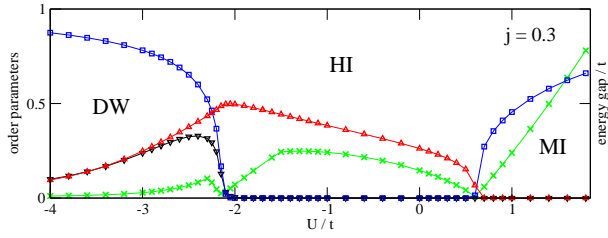


FIG. 4: Order parameters \mathcal{O}_P^2 (\square), \mathcal{O}_S^2 (\triangle), \mathcal{O}_{DW} (∇), and energy gap (\times) as function of U for constrained bosons on the $j = 0.3$ line ($N = 160$). The parity, as defined in the Mott state, must get an additional oscillating factor in the DW phase $\mathcal{O}_P^2 \rightarrow (-1)^{i-j} \mathcal{O}_P^2$.

where $J = t^2/|U|$. For $j = 0$, this is a $SU(2)$ symmetric chain, whereas the $j^2 J$ terms break the symmetry down to $U(1)$, moving the effective theory obtained after bosonization of $H_{\frac{1}{2}}$ towards the irrelevant direction (in the renormalization group sense). As a result of this, a gapless XY phase of the spin-1/2 chain is expected, i.e. a PSF phase. Higher order terms in $1/|U|$ (not shown explicitly) break, even for $j = 0$, the $SU(2)$ symmetry to $U(1)$ in the irrelevant direction. However, interestingly, the ring exchange along the elementary triangle of the zig-zag chain, with amplitude jt^3/U^2 , forces the effective theory towards the relevant direction, leading to a gapped Néel phase of the spin-1/2 chain, i.e. the DW phase. The competition between exchange along the lattice bonds and ring-exchange leads hence to two consecutive KT phase transitions induced by j , for $j \ll 1$ first from PSF to DW, followed by DW back to PSF. The width of the DW phase is $\sim t/|U|$, and it extends all the way into the $U \rightarrow -\infty$ limit.

Finally, our DMRG simulations show a narrow region where a direct, apparently first-order, HI-PSF transition occurs, characterized by discontinuous jumps of $\mathcal{O}_{S,P}^2$ (Fig. 5). This first-order nature is explained because on one hand increasing $|U|$ within the HI phase increases \mathcal{O}_S^2 due to the suppression of singly-occupied sites, and on the other hand, for $0.6 \lesssim j \lesssim 0.75$ (Fig. 3), a growing $|U|$ destroys the insulating state in favour of a PSF phase, where string order cannot exist. On the contrary, \mathcal{O}_S^2 diminishes for decreasing $|U|$ when approaching the HI-CSF boundary (Fig. 5)

Conclusions. In summary, the interplay between geometrical frustration and interactions leads to rich physics for ultra-cold bosons in zig-zag optical lattices. Unconstrained bosons may present chiral superfluidity, and Mott insulator for vanishingly small interactions. Constrained bosons may allow for the observation of Haldane-insulator without the necessity of polar interactions, as well as pair-superfluid and density wave phases at attractive interactions. All the predicted phases may be detected using state of the art techniques. The SF and CSF phases may be distinguished by means of time-of-flight (TOF) techniques, in a similar way as recently done

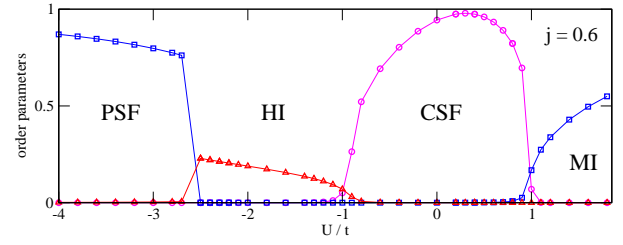


FIG. 5: Order parameters \mathcal{O}_P^2 (\square), \mathcal{O}_S^2 (\triangle), and κ^2 (\circ) as function of U for constrained bosons on the $j = 0.6$ line ($N = 160$). Both $\mathcal{O}_{P,S}^2$ show jumps at the HI to PSF transition at $U \simeq -2.5$. In the PSF, similar to the DW phase, \mathcal{O}_P^2 is defined with an additional oscillating factor.

for condensates in triangular optical lattices [7]. The DW and PSF phases are characterized by double or zero occupancy, which could be detected using parity measurements as those introduced in Refs [32, 33], and could be discerned from each other by the absence/presence of interference fringes in TOF [34]. Finally, the string-order of the HI phase may be studied using similar site-resolved measurements as those recently reported for the measurement of non-local parity order in Mott insulators [20].

This work has been supported by the cluster of excellence QUEST (Center for Quantum Engineering and Space-Time Research). T.V. acknowledges SCOPES Grant IZ73Z0-128058.

-
- [1] M. Lewenstein *et al.*, Adv. in Phys. **56**, 243 (2007).
 - [2] C. Becker *et al.*, New J. Phys. **12**, 065025 (2010).
 - [3] G.-B. Jo *et al.*, Phys. Rev. Lett. **108**, 045305 (2012).
 - [4] S. D. Huber and E. Altman, Phys. Rev. B **82**, 184502 (2010).
 - [5] A. Eckardt, C. Weiss, and M. Holthaus, Phys. Rev. Lett. **95**, 260404 (2005).
 - [6] A. Zenesini *et al.*, Phys. Rev. Lett. **102**, 100403 (2009).
 - [7] J. Struck *et al.*, Science **333**, 996 (2011).
 - [8] C. Chin *et al.*, Rev. Mod. Phys. **82**, 1225 (2010).
 - [9] A. J. Daley *et al.*, Phys. Rev. Lett. **102**, 040402 (2009).
 - [10] I. Titvinidze *et al.*, New Journal of Physics **13**, 035013 (2011).
 - [11] L. Bonnes and S. Wessel *et al.*, Phys. Rev. Lett. **106**, 185302 (2011).
 - [12] Y.-C. Chen, K.-K. Ng, and M.-F. Yang, Phys. Rev. B **84**, 092503 (2011).
 - [13] M. J. Mark *et al.*, arXiv:1201.1008.
 - [14] E. G. Dalla Torre, E. Berg, and E. Altman, Phys. Rev. Lett. **97**, 260401 (2006).
 - [15] T. Lahaye *et al.*, Rep. Prog., Phys. **72**, 126401 (2009).
 - [16] F. D. M. Haldane, Phys. Lett. A **93**, 464 (1983); Phys. Rev. Lett. **50**, 1153 (1983).
 - [17] E. Berg *et al.*, Phys. Rev. B **77**, 245119 (2008).
 - [18] M. den Nijs, and K. Rommelse, Phys. Rev. B **40**, 4709 (1989).
 - [19] T. Giamarchi, *Quantum Physics in One Dimension*, Oxford University Press (2003).
 - [20] M. Endres *et al.*, Science **334**, 200 (2011).

- [21] A. A. Nersesyan, A. O. Gogolin, and F.H.L. Essler, Phys. Rev. Lett. **81**, 910 (1998).
- [22] See supplementary material for details.
- [23] One may map boson problem by means of the Holstein-Primakoff transformation $S_i^z = 1 - n_i$, $S_i^+ = \sqrt{2 - n_i}$ to frustrated spin-1 XY chain (up to particle-hole symmetry breaking terms that are irrelevant [17]), $H_S = t \sum_i [(\vec{S}_i \cdot \vec{S}_{i+1})_{XY} + j(\vec{S}_i \cdot \vec{S}_{i+2})_{XY} + D(S_i^z)^2]$, where $(\vec{S}_i \cdot \vec{S}_j)_{XY} \equiv S_i^x \cdot S_j^x + S_i^y \cdot S_j^y$, and $D = U/4t$ and j characterize, respectively, the single-ion anisotropy and the next-nearest neighbor frustrating exchange.
- [24] Numerically we have unambiguously confirmed the Ising nature of SF-PSF transition by observing the correct scaling of \mathcal{O}_P^2 close to transition point.
- [25] S. R. White, Phys. Rev. Lett. **69**, 2863 (1992); Phys. Rev. B **48**, 10345 (1993); U. Schollwöck, Rev. Mod. Phys. **77**, 259 (2005).
- [26] It is notoriously hard to determine precisely the KT phase transition lines by this method alone. The precise location of the phase transition lines, and the determination of the nature of the multi-critical points close to $j = 0$ are not pursuit in the current work.
- [27] A. K. Kolezhuk, Prog. Theor. Phys. Suppl. **145**, 29 (2002); Phys. Rev. B **62**, R6057 (2000).
- [28] T. Hikihara *et al.*, J. Phys. Soc. Jpn. **69**, 259 (2000).
- [29] T. Hikihara, J. Phys. Soc. Jpn. **71**, 319 (2002).
- [30] H.J. Schulz, Phys. Rev. B **34**, 6372 (1986).
- [31] T. Vekua, et al, Phys. Rev. B **76**, 174420 (2007).
- [32] W. S. Bakr *et al.*, Science **329**, 547 (2010).
- [33] J. F. Sherson *et al.*, Nature **467**, 68 (2010).
- [34] M. Greiner *et al.*, Nature **415**, 39 (2002).

Supplementary material to “Ultra-cold bosons in zig-zag optical lattices ”

S. Greschner,¹ L. Santos,¹ and T. Vekua¹

¹*Institut für Theoretische Physik, Leibniz Universität Hannover, 30167 Hannover, Germany*

In this supplementary material, we provide some additional details on the bosonization description of the possible sequential CSF-CMI-MI phase transitions for $j > 1/4$. As mentioned in the main text, in the $j \gg 1$ regime we may consider sub-chains formed by the even and odd sites, and introduce the symmetric and antisymmetric fields θ_{\pm} and ϕ_{\pm} . The interaction between these fields is given by the last two terms of Eq. (3) of the main text:

$$\mathcal{H}_{int} = \lambda \partial_x \theta_+ \sin \sqrt{2\pi} \theta_- - 2\mathcal{M} \cos \sqrt{2\pi} \phi_+ \cos \sqrt{2\pi} \phi_-, \quad (1)$$

where the first term supports chirality and the second one favors a MI phase.

Starting from $U \gg t'$, deep in the Mott phase of each sub-chain, then $\langle \cos \sqrt{2\pi} \phi_{\pm} \rangle \neq 0$, and thus the ϕ_{\pm} fields are pinned in the Mott phase. In this case, to second order in λ , one can integrate out in the partition function $\partial_x \theta_+$ from the first term of Eq.(1), obtaining the following contribution in the antisymmetric sector,

$$-\frac{\lambda^2}{2} \int d^2x d^2y \langle \partial_x \theta_+ \partial_y \theta_+ \rangle \sin \sqrt{2\pi} \theta_-(x) \sin \sqrt{2\pi} \theta_-(y)$$

where the average is performed in the ground state of the MI phase, where $\langle \partial_x \theta_+ \partial_y \theta_+ \rangle$ is short ranged. Hence the leading contribution in the antisymmetric sector, after carrying out operator product expansion, is a term $\sim \lambda^2 \cos \sqrt{8\pi} \theta_-$. Note that a $\sim -\lambda^2 (\partial_x \theta_-)^2$ contribution decreasing the value of K_- is obtained as well in the antisymmetric sector. The competition between $\cos \sqrt{8\pi} \theta_-$ and $\cos \sqrt{2\pi} \phi_-$ (obtained using mean-field decoupling of the last term of Eq.(1) in the MI phase) is resolved with an Ising phase transition in the antisymmetric sector with increasing λ/U , leading to the pinning of θ_- in the new ground state $\langle \sqrt{8\pi} \theta_- \rangle = \pi$, so that $\langle \sin \sqrt{2\pi} \theta_- \rangle \neq 0$, driving the symmetric sector into a state with finite topological current, $\langle \partial_x \theta_+ \rangle \neq 0$.

The simplest scenario to establish the Ising phase transition is for $K_- = 2$. In that case, performing a mean-field decoupling of the second term in Eq. (1), the antisymmetric sector is governed by the Hamiltonian density,

$$\mathcal{H}_- = \frac{v_-}{2} [(\partial_x \tilde{\phi}_-)^2 + (\partial_x \tilde{\theta}_-)^2] - \tilde{M} \cos \sqrt{4\pi} \tilde{\phi}_- + \tilde{\lambda} \cos \sqrt{4\pi} \tilde{\theta}_-,$$

where $\tilde{\theta}_- = \sqrt{K_-} \theta_-$, $\tilde{\phi}_- = \phi_- / \sqrt{K_-}$, $\tilde{M} = 2\mathcal{M} \langle \cos \sqrt{2\pi} \phi_+ \rangle$, and $\tilde{\lambda} \sim \lambda^2$. The antisymmetric sector can be hence described by two free massive Majorana fermions, with masses $\tilde{\lambda} \pm \tilde{M}$. At the Ising phase transition, $\tilde{\lambda} = \pm \tilde{M}$, and the mass of one of the Majorana fermions vanishes [1].

However, the Mottness of the ground state after the chirality gets long-range ordered, $\langle \sqrt{2\pi} \theta_- \rangle \neq 0$, does not necessarily disappear immediately, due to the possibility of a relevant contribution in the symmetric sector, $\cos \sqrt{8\pi} \phi_+$, for $K_+ < 1$ which stems after integrating out the $\cos \sqrt{2\pi} \phi_-$ in the last term of Eq. (1) in the state with pinned θ_- . Note that in the CMI state $\langle \theta_- \rangle \neq 0$, $\langle \partial_x \theta_+ \rangle \neq 0$, and also $\langle \phi_+ \rangle \neq 0$. Further decreasing U , at $K_+ = 1$, the CMI phase ($K_+ < 1$) disappears at a KT phase transition in favor of the CSF phase ($K_+ > 1$).

Thus, our bosonization analysis, for $j \gg 1$, suggests the possibility of two consecutive phase transitions with increasing U starting from the CSF phase, first a KT transition from CSF to CMI, followed by the Ising phase transition from CMI to MI.

-
- [1] A.O. Gogolin, A. A. Nersesyan, and A. M. Tsvelik, *Bosonization and Strongly Correlated Systems*, Cambridge University Press (1998).